AAAS
Space: Science & Technology
Volume 2021, Article ID 9835728, 13 pages
https://doi.org/10.34133/2021/9835728

Space: Science & Technology
A SCIENCE PARTNER JOURNAL

Research Article

Investigation on P-Glycoprotein Function and Its Interacting Proteins under Simulated Microgravity

Yujuan Li,[1] **Lili Huang**,[1] **Javed Iqbal**,[2] **and Yulin Deng**[1]

[1]*School of Life Sciences, Beijing Institute of Technology, Beijing 100081, China*
[2]*Department of Biology, Government College Mankera, University of Sargodha, Sargodha, Pakistan*

Correspondence should be addressed to Yujuan Li; lylyjlzh2006@163.com and Yulin Deng; deng@bit.edu.cn

Received 1 February 2021; Accepted 30 April 2021; Published 17 June 2021

P-glycoprotein (P-gp) could maintain stability of the nerve system by effluxing toxins out of the blood-brain barrier. Whether it plays a very important role in drug brain distribution during space travel is not yet known. The present study was aimed at investigating P-gp function, expression, and its interacting proteins in a rat brain under simulated microgravity (SMG) by comparative proteomics approach. Rats were tail-suspended to induce short- (7-day) and long-term (21-day) microgravity. P-gp function was assessed by measuring the P-gp ATPase activity and the brain-to-plasma concentration ratio of rhodamine 123. P-gp expression was evaluated by Western blot. 21d-SMG significantly enhanced P-gp efflux activity and expression in rats. Label-free proteomics strategy identified 26 common differentially expressed proteins (DEPs) interacting with P-gp in 7d- and 21d-SMG groups. Most of the DEPs mainly regulated ATP hydrolysis coupled transmembrane transport and so on. Interaction analysis showed that P-gp might potentially interact with heat shock proteins, sodium/potassium ATP enzyme, ATP synthase, microtubule-associated proteins, and vesicle fusion ATPase. The present study firstly reported P-gp function, expression, and its potentially interacting proteins exposed to simulated microgravity. These findings might be helpful not only for further study on nerve system stability but also for the safe and effective use of P-gp substrate drugs during space travel.

1. Introduction

Space traveling is becoming more and more attractive and inevitable with the development of manned spaceflights for deep space studies. However, there are many hostile limiting factors in space environment such as consistent microgravity, strong radiation, and noise, which could cause various pathophysiological changes of astronauts [1–3]. Lots of available literatures indicate that exposure to microgravity leads to dysfunction of the nerve and cardiovascular system, bone loss, muscle atrophy, energy metabolism disorder of the liver, and destruction of the intestinal mucosa [4–9]. Injury of the nerve system would reduce the performance of astronauts in space, and even their health is at high risk [4, 10–12]. Microgravity can also cause many diseases such as space motion sickness vomiting and many others [13, 14]. To avoid such health problems during space traveling, drugs were administered to relieve the uncomfortable feelings of astronauts [15, 16]. However, it has been observed that pharmacokinetics (PK) of some drugs could significantly be changed under simulated microgravity [17, 18]. This might affect the efficacy of drugs and lead to unexpected outcomes [19, 20]. An accurate amount of drug that should be delivered into the brain is becoming a key problem.

P-gp is an ATP-dependent drug transport protein, and it is predominantly found in the apical membranes of a few endothelial and epithelial cell types in the body, including the blood luminal membrane of the brain capillary endothelial cells that make up the blood–brain barrier (BBB) [21, 22]. P-gp at the BBB could efflux its substrate drugs and limit the entry of substrates into the brain. As P-gp protects the brain from many exogenous toxins, P-gp dysfunction would change brain penetration of many drugs, which may lead to changed effects of the drugs on the central nerve system (CNS) or increased adverse effects [23]. For treatment of CNS disorders, drug transport across the BBB needs to be achieved to reach efficacy [24, 25]. Emerging evidences suggest that P-gp play important roles in antidepressant and

brain cancer therapy [26, 27]. P-gp is also expressed at the intestine, kidney, and liver. It could affect drug PK behaviors, including drug absorption, distribution, metabolism, and excretion [28, 29]. Alteration of P-gp or its related proteins may change drug PK behaviors under microgravity. However, whether P-gp function at the BBB could be modulated by microgravity remains unclear until today. Reports on P-gp function or its related proteins under microgravity condition are unavailable elsewhere. In order to explore the effect of P-gp and its interacting proteins on brain homeostasis, further study is critically necessary to disclose change of P-gp and its function-related proteins exposed to different microgravity durations.

The present study was aimed at investigating how simulated microgravity (SMG) would affect P-gp function and expression in SMG rat brain and screening its interacting proteins based on a label-free comparative proteomics method. Rats were tail-suspended to simulate microgravity according to the Morey-Holton model, a frequently used and well-accepted ground analog approved by the National Aeronautics and Space Administration (NASA) [30].

2. Materials and Methods

2.1. Reagents. Radioimmunoprecipitation assay (RIPA) lysis buffer, protease inhibitor, secondary horseradish peroxidase-(HRP-) conjugated goat anti-rabbit IgG, rabbit monoclonal P-gp, rabbit sodium/potassium-transporting ATPase subunit beta-1 (Atp1b1) antibody, and trypsin were purchased from Abcam Company (MA, USA). Protein A/G Plus-Agarose was supplied by Santa Cruz Biotechnology Company (CA, USA). Acetonitrile and formic acid were of chromatographic grade from Thermo Fisher Scientific Inc. (MA, USA). Bicinchoninic acid (BCA) protein assay kit was purchased from Bio-Rad Company (CA, USA). 3-[(3-Cholamidopropyl) dimethylammonio]-1-propanesulfonate (CHAPS) and Rhodamine 123 (Rho123) were purchased from Bailingwei Scientific and Technology Company (Beijing, China). The ultra-micro-ATPase test box was supplied by Nanjing Jiancheng Company (Nanjing, China).

2.2. Animals and Development of the Morey-Holton Model. All animal procedures complied with the Guide for the Care and Use of Laboratory Animals published by the National Institutes of Health (NIH publication no. 85-23, revised in 1985). All experiments were approved by Beijing Institute of Technology Animal Care and Use Committee (SYXK-BIT-20200109002). Sprague-Dawley rats (male, SPF, 180-220 g, ten-week-old) were obtained from Academy of Military Medical Sciences (Beijing, China). Rats were raised in a temperature- and humidity-controlled room (temperature $24 \pm 1^{\circ}$C, humidity $55 \pm 5\%$) with an artificial 12 h light-dark cycle and had free access to water and normal standard chow diet. All the animals were kept in such room to acclimate with the environment for one week prior to the study.

The rats were randomly divided into three groups with nine rats in each group including one control (CON) group that was kept on the ground. Rats in the other two groups were tail-suspended for 7 and 21 days (marked as 7d- and 21d-SMG groups) to induce the simulated microgravity according to the Morey-Holton model [30]. Briefly, a surgical tape was wrapped around the rat's tail and connected to a pulley by a metal bar. The tilt angle was between -30° and -35° in relation to the horizontal. It was ensured that the rats could freely move in their cages and had free access to water and food. At the end of due time, all the rats were anaesthetized with 10% chloral hydrate (350 mg/kg), and blood samples were collected. Then, rats were sacrificed by heart perfusion (0.9% saline). Rat brain tissues were collected and kept at –80°C for further experiments.

2.3. Western Blot Analysis. Rat brain samples were collected following the methods in Section 2.2. P-gp expression in CON, 7d-SMG, and 21d-SMG groups was determined by Western blot. For Western blot, the protein concentration was measured with the BCA Protein Assay Kit. Equal amount of protein in each group was separated using 12% SDS-PAGE and transferred to polyvinylidene fluoride (PVDF) membranes (Bio-Rad, CA, USA). Membranes were blocked in 3% BSA-Tris-buffered saline (TBS) for 2 h and then was incubated with appropriate primary antibody (P-gp, 1 : 5000 dilution) for overnight at 4°C. After membranes were washed three times with TBST buffer, appropriate secondary antibodies labeled with HRP were added and incubated at room temperature for 2 h. Then, membranes were washed three times with TBS again; immunoblots were visualized with enhanced chemiluminescence (ECL) reaction (Amsterdam, NL) reagents, followed by exposing to Gel Doc XR system (Bio-Rad Laboratories, CA, US). The density of each band was quantitated by Chemi High-Resolution Imaging System and Odyssey application software (LI-COR Biosciences, Lincoln, NE).

2.4. P-gp Function Assessment. P-gp function was measured by ATPase activity of P-gp and Rhodamine 123 (Rho123) distribution in the rat brain. To elucidate the effect of SMG on P-gp transport function at the BBB, Rho123 (0.2 mg/kg), a typical substrate of P-gp, was injected intravenously to rats of CON and SMG groups. At 60 min after the injection of Rho123, the rats were sacrificed under sodium pentobarbital anesthesia, and then, blood was immediately collected into heparinized tubes to get plasma samples. After rat heart perfusion was performed with saline, brain tissue was collected. For Rho123 determination, 0.1 g of brain tissue was homogenized in 0.9 mL of saline. Plasma samples and brain homogenates were centrifuged at 12000 × g for 10 min. 100 μL of each supernatant was mixed with 100 μL of saline and 300 μL of methanol, and then, the mixture was vortexed for 30 s. The mixture was centrifuged at 15000 × g for 10 min. 100 μL of supernatant was used for assay of Rho123 in rat plasma and brain samples by fluorescence intensity. Excitation and emission wavelengths were 495 and 530 nm, respectively [31]. The brain-to-plasma concentration ratio of Rho123 was calculated for assessment of P-gp efflux function in the rat brain.

As P-gp transports its substrate, ATP is hydrolyzed and inorganic phosphorate is produced as a byproduct. The

ATPase activity of P-gp in mammalian cell membranes is vanadate sensitive [32]. According to the difference of the amount of inorganic phosphorate production induced by the samples in the presence or absence of P-gp-related ATPase inhibitor vanadate, P-gp-related ATPase activity was measured. The released phosphate can be determined by a sensitive colorimetric reaction. The experimental operation followed a previously published protocol [33]. Briefly, 0.1 g of brain tissue was homogenized in 0.9 mL of saline, and then, the homogenate was centrifuged at 2500 rpm for 10 min. The supernatant was diluted with saline to get a 0.05% final sample concentration (the ratio of brain tissue weight to volume of saline). 250 μL of each sample was added to the Microplate Reader (Thermo Multiskan Ascent, Thermo Company, USA), and the absorbance was measured at 636 nm. P-gp function of samples was calculated following the instructions of the ultra-micro-ATPase test kit and was expressed as unit/milligram protein.

2.5. Coimmunoprecipitation (Co-ip) Assay and In-Gel Digestion. About 0.5 g of each brain sample was homogenized in RIPA containing 1% CHAPS and protease inhibitors. The homogenate was centrifuged at 3000 × g for 10 min at 4°C, and the resulting supernatant fractions were collected. The total protein concentration in the supernatant was measured by BCA protein assay kit. Protein concentration of nine samples from the CON group was adjusted to be the same level. An equal volume of every three samples in the CON group was taken and mixed to get three final samples for the CON group. 7d- and 21d-SMG samples were made to follow the same method from the 7d- and 21d-SMG groups, respectively. The final control group sample was divided into two groups named as CON and negative CON groups, respectively. Samples incubated with IgG served as the negative control. Taken together, samples from CON, negative CON, 7d-SMG, and 21d-SMG groups were obtained finally for the next coimmunoprecipitation (Co-ip) procedure.

300 μg of proteins from the above four groups was incubated with 30 μL of Protein A/G Plus-Agarose at 4°C for 2 h. After centrifugation (3000 rpm, 1 min) was performed at 4°C, the resulting supernatants were collected into clear tubes. 2 μg of the P-gp antibody was added into CON, 7d-SMG, and 21d-SMG groups. 2 μg of IgG was added into the negative control group. After the above four group samples were kept overnight at 4°C, samples were incubated with 30 μL of Protein A/G Plus-Agarose at 4°C for 6 h. Then, samples were centrifuged (3000 rpm, 1 min) at 4°C to collect the precipitations. The precipitations were gently washed twice with 1 mL of PBS; then, centrifugation was repeated. After the supernatant was discarded, Co-ip complex and IgG-negative CON complex were collected. 15 μL of loading buffer was added into the complex and then incubated in boiled water for 10 min. The supernatant was collected after centrifugation (3000 rpm for 1 min) at 4°C.

The proteins in the Co-ip complex from each sample were separated by 12% sodium dodecyl sulfate-polyacrylamide gel electrophoresis (SDS–PAGE). After separation was completed, the gel was stained with Brilliant Blue G (Solarbio Company, Beijing, China) for 1 h. The stained gel was washed with 20% methanol repeatedly until the bands were clear. For in-gel digestion, each lane of the gel was cut into four slices with a clear knife and slices were transferred into clear tubes. Briefly, in-gel digestion procedures mainly included destaining of gel slices, protein reduction and alkylation, and digestion of proteins. A detailed protocol followed published literatures [9] with slight modification. After digestion, peptides were dried by vacuum concentration and diluted in 3% acetonitrile and 0.1% formic acid aqueous solution. The dried peptides were stored at -20°C before use.

2.6. LC-MS/MS Analysis. The peptides from four groups were separated by reverse phase chromatography column (3 μm, 150 mm ×75 μm, Eksigent) with an Eksigent 1D-Ultra Nanoflow High-Performance Liquid Chromatography (HPLC) system coupled to a Sciex 4600 Q-TOF mass spectrometer (Agilent, USA). The mobile phase consisting of solvent A (acetonitrile with 0.1% formic acid) and solvent B (water with 0.1% formic acid) was delivered under the linear gradient from 2% A to 98% A within 100 min at a flow rate of 300 nL/min. 98% A was kept until 120 min for one complete chromatographic run.

The Q-TOF mass spectrometer parameters were as follows: positive ionization mode; capillary voltage, 2300 V; temperature of drying gas, 325°C; curtain gas, 15 Psi; ion source gas, 8 Psi; flow rate, 5.0 L/min; and ion fragmentary voltage, 175 V. The MS scan range was from 350 to 1250 m/z with a scan rate of 1st spectra/sec. MS/MS spectrum scan range was m/z 100-1250. The top five precursor ions in the MS scan were selected for subsequent auto-MS/MS scans and dynamic exclusion time of 25 s. IDA automatic mode was used for acquisition of MS/MS.

2.7. Protein Identification and Bioinformatics. MS/MS data analysis was achieved using PEAKS Studio software (Version 6.0, Bioinformatics Solutions, Waterloo, Canada) with the SwissProt database (http://www.uniport.org/downloads), which included 33563 sequences of *Rattus norvegicus*. The carbamidomethylation of cysteine was chosen for the fixed modification; oxidation of methionine was considered as variable modification. Trypsin was used as a digestion enzyme, and two missed cleavages were allowed. Peptide mass tolerance and fragment mass tolerance were 15 ppm and 50 ppm, respectively. Peptides were identified if the probability of a false discovery rate (FDR) was less than 1%. Only proteins with at least two peptides meeting the criteria were selected for protein identification. Proteins would be used for further analysis only when at least two out of three technical replicates were identified in mass spectrum.

In order to eliminate the interference of IgG, proteins from CON, 7d-SMG, and 21d-SMG groups were compared with the negative CON group first. If identified proteins were not found in the negative CON group or the ratio of identified proteins in CON, 7d-SMG, and 21d-SMG groups to that in the negative CON group was more than 10 times, such proteins were preserved for further differential proteomics analysis. After the IgG background correction, the ratio of protein intensity in the 7d- and 21d-SMG group to that in the CON group was defined as fold change. Proteins were

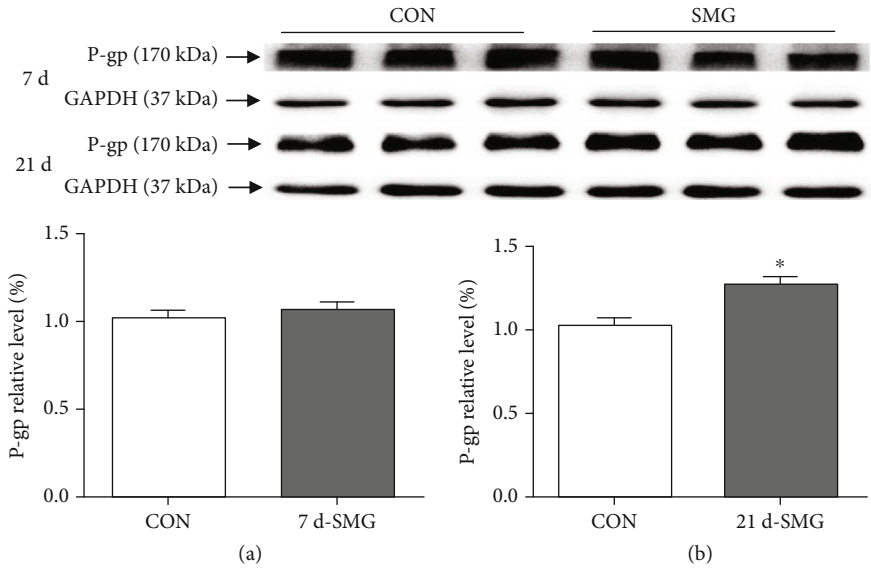

Figure 1: Quantification of P-gp in the rat brain by Western blot in the 7d-SMG group ((a), $n = 9$) and 21d-SMG group ((b), $n = 9$). Compared with CON, $^{*}P < 0.05$.

selected as differentially expressed proteins (DEPs) when their fold changes were more than 2 (upregulation) or less than 0.5 (downregulation) and P value was less than 0.05. Then, DEPs were analyzed by DAVID Bioinformatics tool (version 6.7) and PANTHER classification system (version 15.0). The STRING database (version 11.0) was used to search for the networks of DEPs significantly interacting with P-gp between CON and SMG groups [34]. Expression of P-gp and ATP1b1 in the Co-ip complex from CON, negative CON, 7d-SMG, and 21d-SMG groups was determined by Western blot (method in Section 2.3) to validate the Co-ip procedure and MS data, respectively.

2.8. Statistical Analysis. Data were expressed as mean ± SD from at least three independent experiments. Statistical analysis for Western blot and P-gp function test was performed using SPSS 20.0 software (IBM, Armonk, USA). Difference between groups was determined by one-way analysis of variance (ANOVA). A P value less than 0.05 was considered statistically significant.

3. Results

3.1. Expression of P-gp by Western Blot. The P-gp expression level in the brain of CON and SMG rats was measured using Western blot (Figure 1). The result revealed a band of 170 kDa corresponding to P-gp. The P-gp expression level in 21d-SMG rats was significantly ($P < 0.05$) higher than that in CON rats, inducing a 20.4% increase on average. There was no remarkable alteration for the P-gp expression in 7d-SMG rats. Immunohistochemistry (IHC) assay was also used to demonstrate the expression of P-gp in the brain of CON and SMG rats, and the results are shown in Figure 2. The staining area of P-gp was significantly increased after 21d-SMG, which was consistent with the result of Western blot. The increased P-gp expression in the 21d-SMG group was in a good agreement with the increased of P-gp ATPase activity and decreased amount of Rho123 level in the rat brain. An enhanced P-gp function may result from the increase of P-gp expression and P-gp ATPase activity in the rat brain.

3.2. P-gp Function Analysis. Rho123 was used for evaluating P-gp function at the BBB. The ratios of brain-to-plasma Rho123 concentration in CON and SMG rats after intravenous dose was calculated (data is shown in Table 1). The ratios in the CON and 7d-SMG groups were 0.514 ± 0.09 and 0.568 ± 0.04, respectively. 7d-SMG did not significantly alter brain-to-plasma ratio of Rho123 ($P > 0.05$). The ratios in the CON and 21d-SMG groups were 0.524 ± 0.04 and 0.428 ± 0.05, respectively. 21d-SMG significantly decreased Rho123 concentrations in the rat brain ($P < 0.05$). Tissue to plasma concentration ratios in 21d-SMG rats decreased by 18.3%.

P-gp ATPase activity in the rat brain from the CON and 7d-SMG groups was 18.06 ± 2.8 and 19.17 ± 4.8 U/mgprot. In the CON and 21d-SMG groups, P-gp ATPase activity was 60.92 ± 11.5 and 67.45 ± 4.2 U/mgprot. Compared with the CON group, 21d-SMG induced a dramatic increase in P-gp ATPase activity in the rat brain ($P < 0.05$). No significant change was observed in the 7d-SMG group. The decreased amount of Rho123 and increased P-gp ATPase activity in rats exposed to 21d-SMG indicated that P-gp efflux function was dramatically enhanced, while short-term 7d-SMG duration did not significantly influence P-gp function.

3.3. Differentially Expressed Proteins (DEPs) Interacting with P-gp. Compared with the CON group, 37 and 38 differentially expressed proteins (DEPs) potentially interacting with P-gp were identified in the 7d- and 21d-SMG groups, respectively (Table 2). The same proteins (26 of DEPs) were

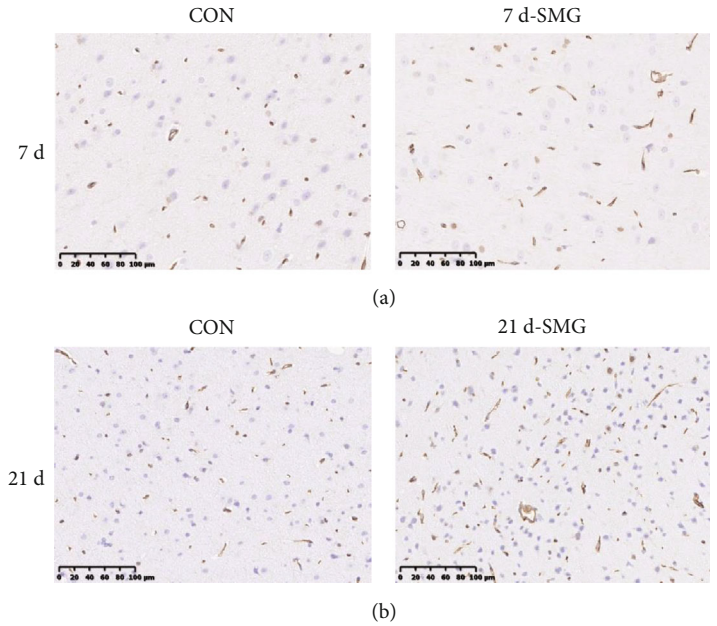

Figure 2: Immunohistochemistry (IHC) of P-gp in the rat brain under 7d-SMG (a) and 21d-SMG (b). The brown dots represent P-gp.

Table 1: The amount of Rho123 in the rat plasma, brain, and the ratio of brain to plasma ($n = 9$).

Duration	Group	Rho123 in brain (ng/g)	Rho123 in plasma (ng/mL)	Ratio of brain to plasma
7 d	CON	26.14 ± 7.45	50.88 ± 9.90	0.514 ± 0.09
	SMG	26.21 ± 4.76	46.13 ± 10.3	0.568 ± 0.04
21 d	CON	18.05 ± 2.56	34.43 ± 3.60	0.524 ± 0.04
	SMG	14.03 ± 1.69*	32.81 ± 6.40	0.428 ± 0.05*

Compared with CON group, $^*P < 0.05$.

selected from both 7d- and 21d-SMG groups. The common proteins are also listed in Table 2. Among these, 21 proteins were consistently downregulated from 7 d to 21 d under SMG. One protein (Thymosin beta-10, Tmsb10) was upregulated in 7d-SMG (with the fold change of 35.4) and remained with a higher expression until 21d-SMG (with the fold change of 74). The rest of the four proteins including 78 kDa glucose-regulated protein (HSPa5), spectrin alpha chain (nonerythrocytic1, Sptan1), Na^+/K^+-transporting ATPase subunit beta-1 (Atp1b1), and alpha-1 (Atp1a1) were first upregulated in the 7d-SMG group and then downregulated in the 21d-SMG group, showing an inconsistent expression behavior. Besides common proteins in two groups, 11 and 12 of DEPs were exclusively found in the 7d- and 21d-SMG groups, respectively. Obviously, short- and long-term SMG duration led to a quite different effect on expression of interacted proteins with P-gp in the rat brain.

Atp1b1 (upregulation for the 7d- and downregulation for 21d-SMG group) was analyzed by Western blot in the Co-ip complex to validate the MS data (Figure 3(a)). The result was in accordance with the MS data. Western blot for identification of P-gp in the Co-ip complex is also shown in Figure 3(b), which showed the authenticity of the Co-ip process.

3.4. Protein Functional Annotation

3.4.1. Protein Class of Common Proteins. 26 of DEPs were analyzed with PANTHER bioinformatics tool. Regarding the protein class, DEPs were clustered into 7 groups. Metabolite interconversion enzymes accounted for 27.8% of total DEPs. Transporters and cytoskeletal protein ranked the second place (both were 22.2%, respectively). The rest of the classes were membrane traffic proteins, defense/immunity protein, and structural and translational proteins. Among 26 DEPs, there were 14 phosphodiesterases, which mainly hydrolyze intracellular second messengers like cAMP and cGMP. These second messengers might play an important role in signal transduction of P-gp.

3.4.2. Biological Processes, Cellular Components, and Molecular Functions. To gain more information about P-gp interacting proteins under SMG, protein cluster analysis was performed with the DAVID bioinformatics tool for biological processes (BP), cellular components (CC), and molecular functions (MF), respectively. BP cluster results showed that these 26 DEPs participated in the regulation of various kinds of biological process (Figure 4(a)). According to the fold enrichment (FE) scores, the top five biological processes include

Table 2: Differentially expressed proteins interacted with P-gp under different SMG durations in rat brain.

No.	Protein ID	Protein name	Fold change	
			7 d	21 d
1	P63312	Thymosin beta-10 (Tmsb10)	35.4	74.1
2	P16086	Spectrin alpha chain, nonerythrocytic 1 (Sptan1)	6.27	0.787
3	P06761	78 kDa glucose-regulated protein (Hspa5)	2.62	0.00
4	P06685	Sodium/potassium-transporting ATPase subunit alpha-1 (Atp1a1)	2.12	0.340
5	P07340	Sodium/potassium-transporting ATPase subunit beta-1 (Atp1b1)	2.00	0.00
6	Q9QUL6	Vesicle-fusing ATPase (Nsf)	0.487	0.205
7	O08815	STE20-like serine/threonine-protein kinase (Slk)	0.483	0.00
8	Q5XIF6	Tubulin alpha-4A chain (Tuba4a)	0.428	0.035
9	Q6AXU4	E3 ubiquitin-protein ligase RNF181 (Rnf181)	0.358	0.00
10	P09606	Glutamine synthetase (Glul)	0.322	0.00
11	P61765	Syntaxin-binding protein 1 (Stxbp1)	0.248	0.00
12	P60203	Myelin proteolipid protein (Plp1)	0.122	0.00
13	P20760	Ig gamma-2A chain C region (igg-2a)	0.016	0.001
14	P04797	Glyceraldehyde-3-phosphate dehydrogenase (GAPDH)	0.00	0.00
15	P10719	ATP synthase subunit beta, mitochondrial (Atp5b)	0.00	0.00
16	P15999	ATP synthase subunit alpha, mitochondrial (Atp5a1)	0.00	0.00
17	P48500	Triosephosphate isomerase (Tpi1)	0.00	0.00
18	P51583	Multifunctional protein ADE2 (Paics)	0.00	0.00
19	P62630	Elongation factor 1-alpha 1 (Eef1a1)	0.00	0.00
20	P63039	60 kDa heat shock protein, mitochondrial (Hspd1)	0.00	0.00
21	P69897	Tubulin beta-5 chain (Tubb5)	0.00	0.00
22	Q62865	cGMP-inhibited 3′,5′-cyclic phosphodiesterase A (Pde3a)	0.00	0.00
23	Q63488	Sodium-dependent phosphate transporter 2 (Slc20a2)	0.00	0.00
24	Q6P9T8	Tubulin beta-4B chain (Tubb4b)	0.00	0.00
25	Q99NA5	Isocitrate dehydrogenase [NAD] subunit alpha (Idh3a)	0.00	0.00
26	Q9WVC0	Septin-7 (7-Sep)	0.00	0.00
27	P37377	Alpha-synuclein (Snca)	993.0	—
28	P06302	Prothymosin alpha (Ptma)	906.4	—
29	P04764	Alpha-enolase (Enol)	174.9	—
30	P48721	Stress-70 protein, mitochondrial (Hspa9)	150.9	—
31	P34058	Heat shock protein HSP 90-beta (Hsp90ab1)	120.2	—
32	P04642	L-Lactate dehydrogenase A chain (Ldha)	86.8	—
33	P59215	Guanine nucleotide-binding protein G(o)-alpha (Gnao1)	66.0	—
34	Q6IG01	Keratin, type II cytoskeletal 1b (Krt77)	15.9	—
35	P10111	Peptidyl-prolyl cis-trans isomerase A (Ppia)	6.28	—
36	P45592	Cofilin-1 (Cfl1)	4.51	—
37	P63259	Actin, cytoplasmic 2 (Actg1)	0.429	—
38	Q5M880	PQ-loop repeat-containing protein 1 (Pqlc1)	—	155.6
39	P62628	Dynein light chain roadblock-type 1 (Dynlrb1)	—	24.8
40	P07335	Creatine kinase B-type (Ckb)	—	18.9
41	Q7M767	Ubiquitin-conjugating enzyme E2 variant 2 (Ube2va)	—	3.08
42	P02564	Myosin-7 (Myh-7)	—	0.52
43	P06686	Sodium/potassium-transporting ATPase subunit alpha-2 (Atp1a2)	—	0.00
44	P11442	Clathrin heavy chain 1 (Cltc)	—	0.00
45	P31596	Excitatory amino acid transporter 2 (Slc1a2)	—	0.00
46	P62329	Thymosin beta-4 (Tmsb4x)	—	0.00

Table 2: Continued.

No.	Protein ID	Protein name	Fold change	
			7 d	21 d
47	P63018	Heat shock cognate 71 kDa protein (Hspa8)	—	0.00
48	P85108	Tubulin beta-2A chain (Tubb2a)	—	0.00
49	Q6P9V9	Tubulin alpha-1B chain (Tuba1b)	—	0.00

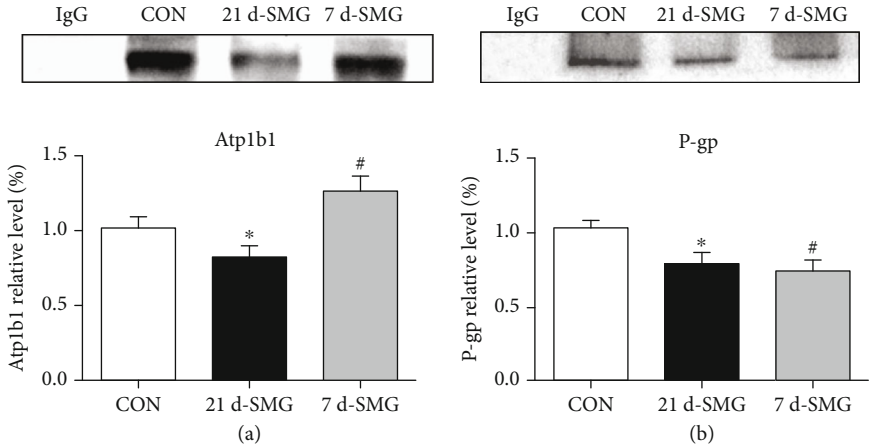

Figure 3: Quantification and validation of the identified proteins in the immunoprecipitation complex: (a) quantification and validation of Atp1b1 ($n = 9$); (b) quantification and validation of P-gp ($n = 9$). $^{*}P < 0.05$ in the 21d-SMG group compared with the CON group; $^{\#}P < 0.05$ in the 7d-SMG group compared with the CON group.

negative regulation of reactive oxygen species biosynthetic process (FE score of 192.7) and ATP hydrolysis coupled transmembrane transport (FE score of 168.6). Membrane repolarization, sodium ion export from cell, and relaxation of cardiac muscle showed the same FE score of 149.9. Besides, cellular potassium ion homeostasis, establishment or maintenance of transmembrane electrochemical gradient, cellular sodium ion homeostasis, ATP hydrolysis and synthesis coupled proton transport, and ATP metabolic process were also enriched in BP.

By cellular component (CC) analysis, the highest FE score in CC was mitochondrial proton-transporting ATP synthase complex, catalytic core F(1) with the FE score of 246.9, followed by sodium/potassium exchanging ATPase complex (FE score of 148.2. FE scores of mitochondrial proton-transporting ATP synthase complex ranked as the third place (67.3). CC analysis results are shown in Figure 4(b). In molecular function (MF) analysis (Table 3), all DEPs were mainly clustered into binding function, accounting for 61% of total DEPs. The binding functions included misfolded protein binding, MHC class I protein binding, syntaxin-1 binding, and potassium ion and sodium ion binding. MF analysis showed that most of the DEPs exhibited binding activities.

From all results of BP, CC, and MF, it could be found that SMG affected ATP hydrolysis coupled transmembrane transport, ATP hydrolysis and synthesis coupled proton transport, and ATP metabolic process, which was related to some proteins including ATP synthase subunit beta (Atp5b), ATP synthase subunit alpha (Atp5a1), and sodium/potassium-transporting ATPase subunit alpha-1 (Atp1a1). P-gp is an ATP-dependent efflux pump, and the transport function of P-gp depends on the binding and the hydrolysis of cytoplasmic ATP within nucleotide binding domains (NBDs) [35, 36]. If ATP synthesis and hydrolysis were disrupted by SMG, P-gp may fail to exhibit efflux function.

3.4.3. Proteins Potentially Interacting with P-gp. P-gp function may be depending on nearby interacting proteins. Interaction analysis was performed by Search Tool for the Retrieval of Interacting Genes/Proteins (STRING 11.0) to analyze potential relation of common proteins with P-gp. The interaction network is shown in Figure 5. P-gp showed potentially direct linkage with glyceraldehyde-3-phosphate dehydrogenase (GAPDH). The references linked in STRING showed interaction between P-gp and GAPDH was based on text mining and coexpression. The interaction results also indicated GAPDH had association with sodium/potassium ATP enzyme (ATP1b1, 1a1), ATP synthase (ATP5b, 5a1), heat shock proteins (HSPd1, HSPa5), elongation factor 1-alpha 1 (Eef1a1), and triosephosphate isomerase (Tpi1), and so on.

Combining all the results from protein functional annotation and information from available literatures, we tried to analyze the potential relation between P-gp and some differentially expressed proteins identified in the present study. The protein network for altered function of P-gp under short- and long-term SMG exposure might be explained.

The protein interaction network showed that heat shock proteins (HSP) could potentially interact with P-gp. Available

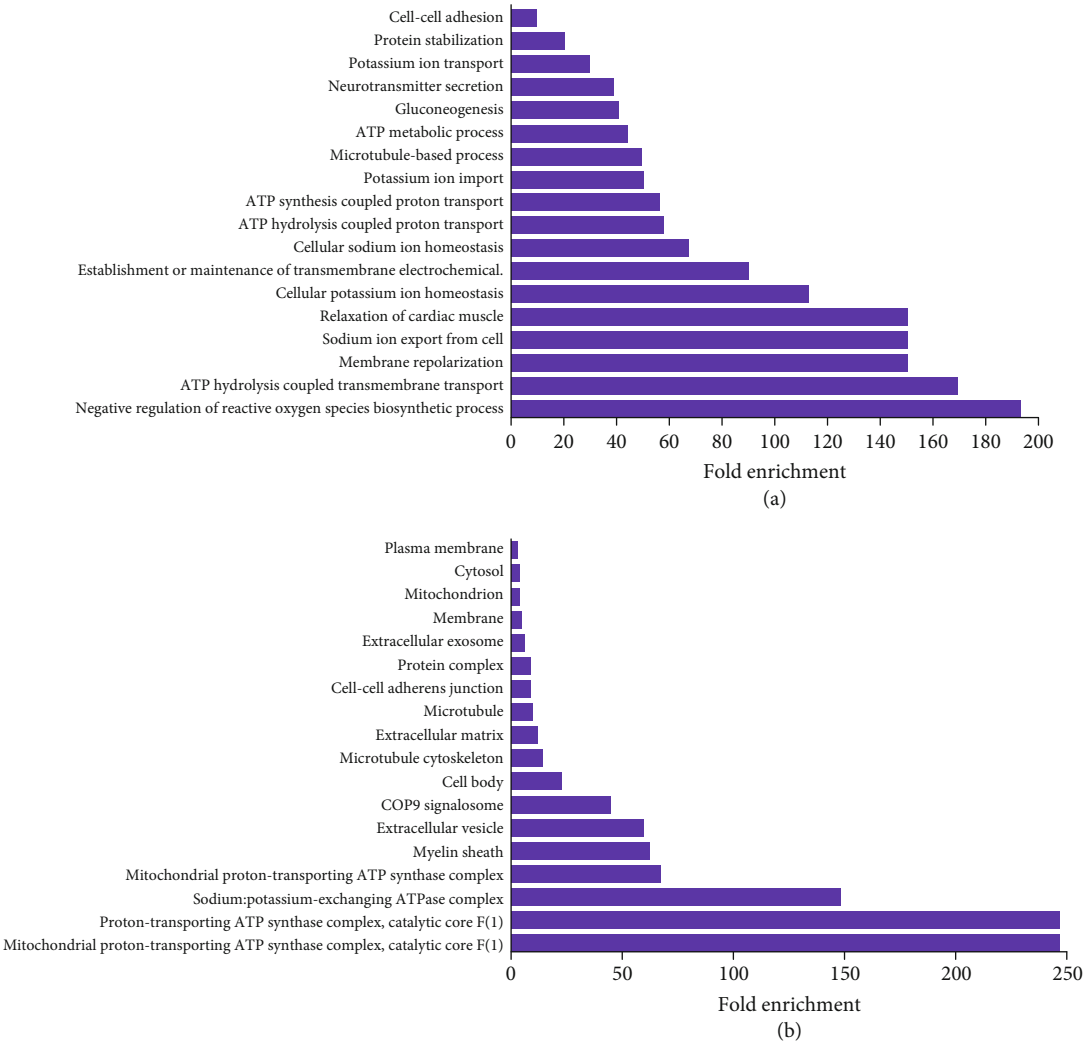

Figure 4: Enriched GO biological process (a) and cellular component (b) of DEPs interacted with P-gp in the SMG rat brain. DEPs were the common proteins from 7d- and 21d-SMG samples.

reports showed that HSP60 could regulate a protective response against toxicity of SMG in SMG-treated nematodes. HSP70 expression was upregulated in endothelial cell after 24 h exposure to SMG. HSP70 upregulation played an important role in the initial adaptive response of endothelial cells to mechanical unloading [37]. Iqbal et al. reported that HSP90α and heat shock cognate 71 kDa protein were increased in the brain of 21d-SMG-treated rats [38]. It has been reported that HSP is linked to cancer cell drug resistance, while P-gp plays a very important role in cancer cell drug resistance [39]. HSPs are directly involved in the expression of multidrug resistance gene-1 (MDR1) or the maturation of P-gp protein conformation in osteosarcoma patients [40]. In P-gp-mediated multidrug resistance, HSP90β is a key regulator of P-gp expression [41]. HSP27 may also participate in the P-gp modulation [40]. In the present study, HSPd1 in the Co-ip complex showed downregulation in both 7d- and 21d-SMG rats, while HSPd5 was upregulated in the 7d-SMG group and downregulated in the 21d-SMG group. P-gp expression in the Co-ip complex from the7d and 21d-SMG groups was downregulated. These results may indicate that HSPs could potentially interact with P-gp. It was speculated that altered HSP expression might modulate the expression of P-gp under SMG condition. Resultantly, the changed P-gp expression may interfere with P-gp efflux function, which may affect the delivery process of substrate drugs while in space.

Vesicle fusion ATPase (Nsf) is another protein that potentially interacted with P-gp. Nsf is abundant in synaptic vesicles and involved in multiple neuronal functions. It could provide chemiosmotic energy for loading neurotransmitters [42] and transport proteins from the endoplasmic reticulum to the Golgi stack [43]. Available reports indicated that Nsf was involved in MDR in some tumors [44]. The gene expression of Nsf was gravity-regulated [45]. Keeping in view the above roles of Nsf, it may be speculated that Nsf could play a role in the process of P-gp transport from the endoplasmic reticulum to Golgi and catalyze the fusion of transport vesicles in Golgi. Compared with the CON group, both the Nsf and P-gp levels in the Co-ip complex of 7d- and 21d-SMG rats were decreased, respectively. Dramatic downregulation

Table 3: Molecular function (MF) analysis of DEPs. Fold enrichment was abbreviated as FE.

No.	Molecular function category	*P* value	FE score
Molecular functions related to binding			
1	Misfolded protein binding	1.9*E*-2	98.5
2	MHC class I protein binding	4.5*E*-4	91.5
3	Syntaxin-1 binding	3.4*E*-2	55.7
4	Potassium ion binding	2.2*E*-2	85.4
5	Sodium ion binding	2.4*E*-2	80.0
6	Syntaxin binding	7.0*E*-3	22.9
7	Ubiquitin protein ligase binding	9.3*E*-3	8.7
8	GTP binding	2.3*E*-3	8.4
9	Protein domain specific binding	1.1*E*-2	8.3
10	Protein complex binding	1.7*E*-2	6.9
11	Identical protein binding	2.4*E*-3	5.9
12	Protein kinase binding	2.7*E*-2	5.8
13	ATP binding	1.2*E*-4	4.6
14	Protein binding	5.2*E*-5	4.4
Molecular functions related to others			
15	Sodium : potassium-exchanging ATPase activity	1.8*E*-2	106.7
16	Proton-transporting ATP synthase activity	2.7*E*-2	71.2
17	Proton-transporting ATPase activity, rotational mechanism	3.7*E*-2	51.2
18	Structural constituent of cytoskeleton	5.2*E*-3	26.7
19	ATPase activity	1.3*E*-4	18.0
20	GTPase activity	3.1*E*-3	12.9
21	Cadherin binding involved in cell-cell adhesion	4.3*E*-2	8.7

of Nsf may affect the transporting function of P-gp in the synthesis process under SMG.

Our results indicated that sodium/potassium ATP enzyme (ATP1b1, 1a1) and ATP synthase (ATP5b, 5a1) were found in the protein interaction network. Current research shows that sodium/potassium ATP enzyme is associated with drug resistance. Targeting sodium/potassium ATP enzyme may become a new way to attack resistant cancer cell with its highly specific ligands [46, 47]. Sodium/potassium ATP enzyme could regulate the expression of multidrug resistant-(MDR-) related genes and P-gp (the product of MDR1) [48]. Stordal et al. reported that sodium/potassium ATP enzyme and MDR might be linked by c-Myc because c-Myc could regulate the expression of MDR and P-gp [49]. These previous findings uncover the association and dependence of P-gp with sodium/potassium ATP enzymes in cells and tissues.

ATP synthase (like ATP5a1 and ATP5b) produces ATP from ADP in the presence of a proton gradient across the membrane. Available reports showed that ATP synthase human lymphocytes and lymphoblastoid cells and ATP level in human Hodgkin's lymphoma cells were decreased by microgravity [50]. P-gp is an ATP-dependent drug transporter. The active drug efflux process is powered by ATP hydrolysis. Decreased ATP synthase and ATP level might change the amount of ATP production, which is not beneficial for P-gp efflux function. In the Co-ip complex of the 7d-SMG group, ATP1a1 and ATP1b1 expression was upregulated compared with the CON group, while 21d-SMG effect downregulated ATP1a1 and ATP1b1 expression. ATP5a1 and ATP5b expression showed downregulation from 7d- and 21d-SMG in the Co-ip complex. A decreased amount of these ATP enzymes might affect P-gp function in the brain under SMG condition, which would possibly change delivery of the administered drugs into the brain during space traveling.

Tubulins play a role in the transport of substances within the cell. Tuba4a, b4b, and b5 showed a possible interaction with P-gp. Tubulins are important part of microtubules which are involved in maintaining the shape and stability of the cells. Studies have shown that expression levels of P-gp and β-tubulin III in ovarian cancer tissues were dramatically increased. Drugs acting on microtubules could promote the expression of P-gp, which could lead to increase in the efflux of drugs [51]. Some multidrug resistance-associated proteins including MRP1 could bind to tubulin through Linker-1 domain [52]. The 5-day flight aboard the Space Shuttle induced the decreased the mRNA levels of alpha-tubulin in rat osteoblasts. Simulated microgravity reduced β-tubulin protein expressions in the K562 cells [53]. It could be speculated that the downregulation of tubulin proteins might affect the expression of P-gp.

4. Discussion

P-gp is highly expressed in brain capillary endothelial cells at the blood brain barrier (BBB) [54]. P-gp at the could efflux its substrate drugs and limit the entry of substrates into the

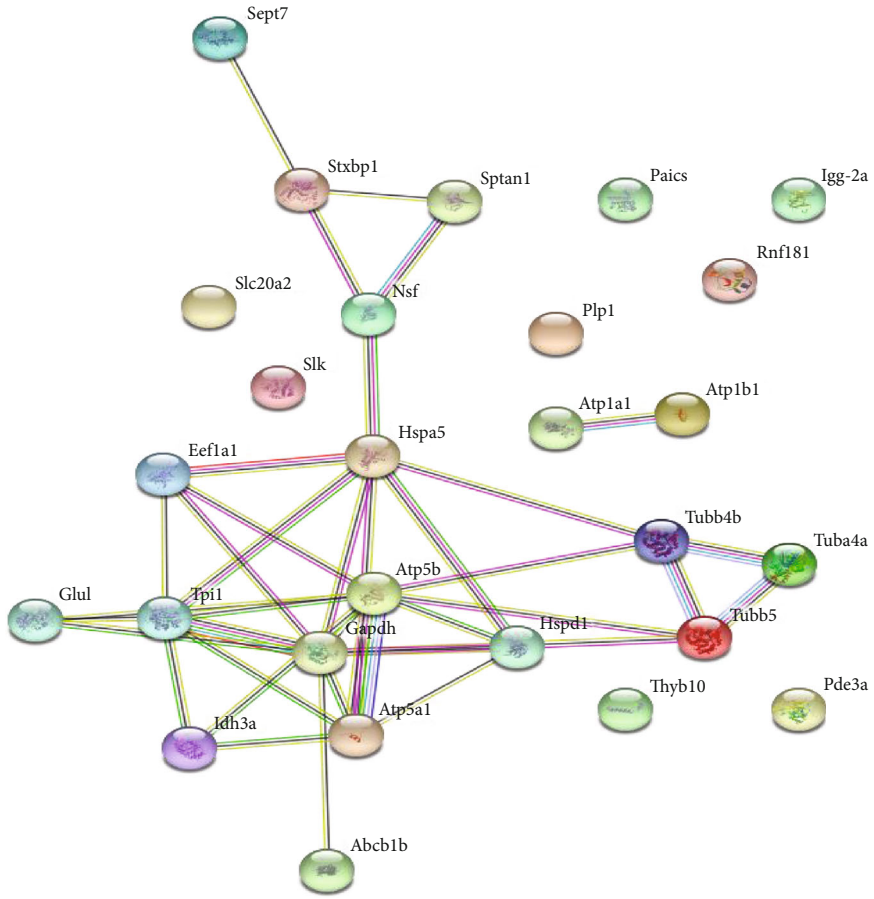

Figure 5: Protein interaction network with P-gp in the 21d-SMG rat brain.

brain. Besides the efflux function of P-gp, it also plays a key role in the barrier function the BBB [29]. Obviously, altered P-gp function under SMG may change effects of the drugs, increase adverse effects [23], or change homeostasis of the central nerve system [29]. Our results indicated that the efflux function and expression of P-gp in the 21d-SMG rat brain have been increased, which implies that drug efficacy or homeostasis of the central nerve system might be influenced. Different SMG periods showed different P-gp function patterns.

In order to screen the underlying protein network interacting with P-gp under SMG condition, 26 DEPs were found in the 7 d and 21 d rat brain samples based on proteomics. It has been found that several proteins including ATP1b1, 1a1, 5b, 5a1, HSPd1, HSPa5, and tubulins may influence P-gp function and expression. Available literatures support that these proteins may have some association with P-gp [37, 39, 45, 51]. It has been reported that Wnt/β-catenin signaling pathways (including p-dvl, p-GSK-3β, GSK-3β, β-catenin, Wnt-3) may regulate the expression of P-gp [55, 56]. However, the present study has found some proteins different from Wnt/β-catenin signaling pathways under SMG. Our results may supply some new information for investigation on P-gp expression and function.

During space travel, drugs were often used to prevent or treat the body injury induced by microgravity. More than 70% of crew members reported the use of a sleep aid (like zolpidem or temazepam) during both short-/long-duration spaceflight missions and International Space Station missions [15, 16]. These drugs are P-gp substrates. Changed P-gp function may alter penetration of its substrate drugs into the brain. At present, astronauts use medications according to the terrestrial medical practices. However, it is not known whether the drugs will act on the body in spaceflight as the same way on Earth or not [57]. P-gp efflux function in the rat brain is increased under 21d-SMG, which may imply that the penetration of P-gp substrate drugs into the brain would be reduced. This may lead to changed efficacy of substrate drugs. Further, P-gp plays an important role in drug absorption in the small intestine and drug excretion in the kidney; thus, more attention should be paid to P-gp function in the small intestine and kidney under microgravity when P-gp substrate drugs are used.

Astronauts use temazepam as sleeping aid in spaceflight missions and International Space Station missions [15, 16]. Analgesics like acetaminophen are used for headaches and pain [58]. It has been reported that temazepam and acetaminophen are substrates of P-gp. P-gp efflux function in the brain may determine the amount of its substrate drugs into the CNS. It was observed that P-gp efflux function in the rat brain was significantly increased under 21d-SMG condition, which may reduce the amount of these CNS drugs

in the brain. Consequently, the pharmacokinetics and/or pharmacodynamics of these CNS drugs possibly would be changed. Drug brain distribution associated with P-gp function under microgravity has been not fully considered. The present study revealed some potentially interacting proteins with P-gp under microgravity. Our findings may provide insight into the protein network of P-gp function exposed to microgravity. It is helpful not only to keep the brain homeostasis of astronauts but also to use CNS drugs effectively and safely during space travel.

It should be noted that the Morey-Holton model is a ground analog to simulate microgravity including fluid shift and muscle atrophy. Fluid shifts in SMG rats may be greater than those in spaceflight rats. Besides, there are some other environmental factors such as radiation during space travel. So, the current findings need to be confirmed in spaceflight. If brain distribution of P-gp substrate drugs was carried out in further study, it would better understand the role of P-gp under microgravity. More efforts should be made in further research on P-gp function, potential mechanism of P-gp, and its interaction proteins.

5. Conclusion

The present study investigated the response of P-gp function and expression to 7d- and 21d-SMG. P-gp interacting proteins in the rat brain were identified by the comparative proteomics approach. 21d-SMG could significantly enhance P-gp efflux function and expression. 26 proteins were found to potentially interact with P-gp. As far as we know, this is the first report on P-gp function and its interacting proteins in the rat brain under simulated microgravity. Our findings are expected to supply some scientific information on medication use safety and nerve system stability during space travel.

Data Availability

The data used to support the findings of this study are available from the author upon request.

Conflicts of Interest

All authors declare no possible conflicts of interests.

Authors' Contributions

Yujuan Li and Yulin Deng participated in the research design. Lili Huang conducted experiments. Lili Huang, Javed Iqbal, and Yujuan Li performed data analysis. Yujuan Li contributed to the writing of the manuscript.

Acknowledgments

This research was financially supported by the National Natural Science Foundation of China (Grant Nos. 81973572 and 81573693) and 1226 Major Project.

References

[1] E. Blaber, H. Marçal, and B. P. Burns, "Bioastronautics: the influence of microgravity on astronaut health," *Astrobiology*, vol. 10, no. 5, pp. 463–473, 2010.

[2] B. Mishra and U. Luderer, "Reproductive hazards of space travel in women and men," *Nature Reviews Endocrinology*, vol. 15, no. 12, pp. 713–730, 2019.

[3] K. Tanaka, N. Nishimura, and Y. Kawai, "Adaptation to microgravity, deconditioning, and countermeasures," *Journal of Physiological Sciences*, vol. 67, no. 2, pp. 271–281, 2017.

[4] X. Mao, L. Sandberg, D. Gridley et al., "Proteomic analysis of mouse brain subjected to spaceflight," *International Journal of Molecular Sciences*, vol. 20, no. 1, p. 7, 2018.

[5] L. K. Pastushkova, D. N. Kashirina, A. G. Brzhozovskiy et al., "Evaluation of cardiovascular system state by urine proteome after manned space flight," *Acta Astronautica*, vol. 160, pp. 594–600, 2019.

[6] J. Yang, Z. Yang, W. Li et al., "Glucocorticoid: a potential role in microgravity-induced bone loss," *Acta Astronautica*, vol. 140, pp. 206–212, 2017.

[7] D. Riva, F. Rossitto, and L. Battocchio, "Postural muscle atrophy prevention and recovery and bone remodelling through high frequency proprioception for astronauts," *Acta Astronautica*, vol. 65, no. 5-6, pp. 813–819, 2009.

[8] B. Chen, J. J. Guo, S. B. Wang, L. T. Kang, Y. L. Deng, and Y. J. Li, "Simulated microgravity altered the metabolism of loureirin B and the expression of major cytochrome P450 in liver of rats," *Frontiers in Pharmacology*, vol. 9, article 1130, 2019.

[9] M. L. Jin, H. Zhang, K. Zhao et al., "Responses of intestinal mucosal barrier functions of rats to simulated weightlessness," *Frontiers in Physiology*, vol. 9, pp. 729–741, 2018.

[10] S. Iwase and T. Mano, "Microgravity and autonomic nervous system," *Japanese Journal of Clinical Medicine*, vol. 58, no. 8, pp. 1604–1612, 2000.

[11] F. Strollo, S. Gentile, G. Strollo, A. Mambro, and J. Vernikos, "Recent progress in space physiology and aging," *Frontiers in Physiology*, vol. 9, p. 1551, 2018.

[12] A. Van Ombergen, A. Demertzi, E. Tomilovskaya et al., "The effect of spaceflight and microgravity on the human brain," *Journal of Neurology*, vol. 264, Supplement 1, pp. 18–22, 2017.

[13] M. Heer and W. H. Paloski, "Space motion sickness: incidence, etiology, and countermeasures," *Autonomic Neuroscience-basic & Clinical*, vol. 129, no. 1-2, pp. 77–79, 2006.

[14] J. R. Lackner and P. Dizio, "Space motion sickness," *Experimental Brain Research*, vol. 175, no. 3, pp. 377–399, 2006.

[15] V. E. Wotring, "Medication use by U.S. crewmembers on the International Space Station," *FASEB Journal*, vol. 29, no. 11, pp. 4417–4423, 2015.

[16] L. K. Barger, E. E. Flynn-Evans, A. Kubey et al., "Prevalence of sleep deficiency and use of hypnotic drugs in astronauts before, during, and after spaceflight: an observational study," *Lancet Neurology*, vol. 13, no. 9, pp. 904–912, 2014.

[17] P. Gandia, S. Saivin, and G. Houin, "The influence of weightlessness on pharmacokinetics," *Fundamental and Clinical Pharmacology*, vol. 19, no. 6, pp. 625–636, 2005.

[18] J. Kast, Y. Yu, C. N. Seubert, V. E. Wotring, and H. Derendorf, "Drugs in space: pharmacokinetics and pharmacodynamics in astronauts," *European Journal of Pharmaceutical Sciences*, vol. 109, pp. S2–S8, 2017.

[19] S. Eyal and H. Derendorf, "Medications in space: in search of a pharmacologist's guide to the galaxy," *Pharmaceutical Research*, vol. 36, no. 10, p. 148, 2019.

[20] J. P. Bagian and D. F. Ward, "A retrospective study of promethazine and its failure to produce the expected incidence of sedation during space flight," *Journal of Clinical Pharmacology*, vol. 34, no. 6, pp. 649–651, 1994.

[21] A. H. Schinkel, "P-glycoprotein, a gatekeeper in the blood-brain barrier," *Advanced Drug Delivery Reviews*, vol. 36, no. 2-3, pp. 179–194, 1999.

[22] K. Yano, T. Tomono, and T. Ogihara, "Advances in studies of P-glycoprotein and its expression regulators," *Biological & Pharmaceutical Bulletin*, vol. 41, no. 1, pp. 11–19, 2018.

[23] J. König, F. Müller, and M. F. Fromm, "Transporters and drug-drug interactions: important determinants of drug disposition and effects," *Pharmacological Reviews*, vol. 65, no. 3, pp. 944–966, 2013.

[24] L. Huang, B. Li, X. Li et al., "Significance and mechanisms of P-glycoprotein in central nervous system diseases," *Current Cancer Drug Targets*, vol. 20, no. 11, pp. 1141–1155, 2019.

[25] K. Linnet and T. B. Ejsing, "A review on the impact of P-glycoprotein on the penetration of drugs into the brain. Focus on psychotropic drugs," *International Journal of Neuropsychopharmacology*, vol. 18, no. 3, pp. 157–169, 2008.

[26] F. E. O'Brien, T. G. Dinan, B. T. Griffin, and J. F. Cryan, "Interactions between antidepressants and P-glycoprotein at the blood-brain barrier: clinical significance of in vitro and in vivo findings," *British Journal of Pharmacology*, vol. 165, no. 2, pp. 289–312, 2012.

[27] S. Agarwal, A. M. Hartz, W. F. Elmquist, and B. Bauer, "Breast cancer resistance protein and P-glycoprotein in brain cancer: two gatekeepers team up," *Current Pharmaceutical Design*, vol. 17, no. 26, pp. 2793–2802, 2011.

[28] C. A. Lee, J. A. Cook, E. L. Reyner, and D. A. Smith, "P-glycoprotein related drug interactions: clinical importance and a consideration of disease states," *Expert Opinion on Drug Metabolism & Toxicology*, vol. 6, no. 5, pp. 603–619, 2010.

[29] M. F. Fromm, "Importance of P-glycoprotein for drug disposition in humans," *European Journal of Clinical Investigation*, vol. 33, Suppl 2, pp. 6–9, 2003.

[30] E. R. Morey-Holton and R. K. Globus, "Hindlimb unloading rodent model: technical aspects," *Journal of Applied Physiology*, vol. 92, no. 4, pp. 1367–1377, 2002.

[31] Y. B. Wang, H. Qin, C. X. Zhang, F. Huan, T. Yan, and L. L. Zhang, "The alterations in the expression and function of P-glycoprotein in vitamin A-deficient rats as well as the effect of drug disposition in vivo," *Molecules*, vol. 21, no. 1, article E46, 2015.

[32] C. Xi, M. Milton, and L.-S. Gan, "Evaluation of drug-transporter interactions using in vitro and in vivo models," *Current Drug Metabolism*, vol. 8, no. 4, pp. 341–363, 2007.

[33] P. Drueckes, R. Schinzel, and D. Palm, "Photometric Microtiter Assay of Inorganic Phosphate in the Presence of Acid- Labile Organic Phosphates," *Analytical Biochemistry*, vol. 230, no. 1, pp. 173–177, 1995.

[34] C. von Mering, M. Huynen, D. Jaeggi, S. Schmidt, P. Bork, and B. Snel, "String: a database of predicted functional associations between proteins," *Nucleic Acids Research*, vol. 31, no. 1, pp. 258–261, 2003.

[35] M. S. Jin, M. L. Oldham, Q. Zhang, and J. Chen, "Crystal structure of the multidrug transporter P-glycoprotein from Caenorhabditis elegans," *Nature*, vol. 490, no. 7421, pp. 566–569, 2012.

[36] S. Mollazadeh, A. Sahebkar, F. Hadizadeh, J. Behravan, and S. Arabzadeh, "Structural and functional aspects of P-glycoprotein and its inhibitors," *Life Sciences*, vol. 214, pp. 118–123, 2018.

[37] P. Liu, D. Li, W. Li, and D. Wang, "Mitochondrial unfolded protein response to microgravity stress in nematode Caenorhabditis elegans," *Scientific Reports*, vol. 9, no. 1, p. 16474, 2019.

[38] J. Iqbal, W. Li, M. Hasan et al., "Distortion of homeostatic signaling proteins by simulated microgravity in rat hypothalamus: A^{16} $O/^{18}$ O-labeled comparative integrated proteomic approach," *Proteomics*, vol. 14, no. 2-3, pp. 262–273, 2014.

[39] F. F. Xu, T. Yang, D. J. Fang, Q. Q. Xu, and Y. Chen, "An investigation of heat shock protein 27 and P-glycoprotein mediated multi- drug resistance in breast cancer using liquid chromatography-tandem mass spectrometry-based targeted proteomics," *Journal of Proteomics*, vol. 108, pp. 188–197, 2014.

[40] S. W. Kim, M. Hasanuzzaman, M. Cho et al., "Casein kinase 2 (CK2)-mediated phosphorylation of Hsp90β as a novel mechanism of rifampin-induced *MDR1* expression," *The Journal of Biological Chemistry*, vol. 290, no. 27, pp. 17029–17040, 2015.

[41] L. E. Cowen and S. Lindquist, "Hsp90 potentiates the rapid evolution of new traits: drug resistance in diverse fungi," *Science*, vol. 309, no. 5744, pp. 2185–2189, 2005.

[42] Y. Moriyama, H. L. Tsai, and M. Futai, "Energy-dependent accumulation of neuron blockers causes selective inhibition of neurotransmitter uptake by brain synaptic vesicles," *Archives of Biochemistry and Biophysics*, vol. 305, no. 2, pp. 278–281, 1993.

[43] S. W. Lorkowski, G. Brubaker, K. Gulshan, and J. D. Smith, "V-ATPase (vacuolar ATPase) activity required for ABCA1 (ATP-binding cassette protein A1)-mediated cholesterol efflux," *Arteriosclerosis, Thrombosis, and Vascular Biology*, vol. 38, no. 11, pp. 2615–2625, 2018.

[44] M. Pérez-Sayáns, J. M. Somoza-Martín, F. Barros-Angueira, P. G. Diz, J. M. G. Rey, and A. García-García, "Multidrug resistance in oral squamous cell carcinoma: the role of vacuolar ATPases," *Cancer Letters*, vol. 295, no. 2, pp. 135–143, 2010.

[45] C. S. Thiel, S. Hauschild, A. Huge et al., "Dynamic gene expression response to altered gravity in human T cells," *Scientific Reports*, vol. 7, no. 1, p. 5204, 2017.

[46] F. Brouillard, D. Tondelier, A. Edelman, and M. Baudouin-Legros, "Drug resistance induced by quabain via the stimulation of MDR1 gene expression in human carcinomatous pulmonary cells," *Cancer Research*, vol. 61, no. 4, pp. 1693–1698, 2001.

[47] T. Mijatovic, F. Dufrasne, and R. Kiss, "Cardiotonic steroids-mediated targeting of the Na^+/K^+-ATPase to combat chemoresistant cancers," *Current Medicinal Chemistry*, vol. 19, no. 5, pp. 627–646, 2012.

[48] T. Mijatovic and R. Kiss, "Cardiotonic steroids-mediated Na +/K+-ATPase targeting could circumvent various chemoresistance pathways," *Planta Medica*, vol. 79, no. 3-4, pp. 189–198, 2013.

[49] B. Stordal, M. Hamon, V. McEneaney et al., "Resistance to paclitaxel in a cisplatin-resistant ovarian cancer cell line is mediated by P-glycoprotein," *PLoS One*, vol. 7, no. 7, article e40717, 2012.

[50] A. J. Jeong, Y. J. Kim, M. H. Lim et al., "Microgravity induces autophagy via mitochondrial dysfunction in human Hodgkin's lymphoma cells," *Scientific Reports*, vol. 8, no. 1, article 14646, 2018.

[51] Y. Jia, S. Sun, X. Gao, and X. Cui, "Expression levels of TUBB3, ERCC1 and P-gp in ovarian cancer tissues and adjacent normal tissues and their clinical significance," *Journal of Buon*, vol. 23, no. 5, pp. 1390–1395, 2018.

[52] R. Ambadipudi and E. Georges, "Sequences in linker-1 domain of the multidrug resistance associated protein (MRP1 or ABCC1) bind to tubulin and their binding is modulated by phosphorylation," *Biochemical and Biophysical Research Communications*, vol. 482, no. 4, pp. 1001–1006, 2017.

[53] Y. Kumei, S. Morita, H. Katano et al., "Microgravity signal ensnarls cell adhesion, cytoskeleton, and matrix proteins of rat osteoblasts: osteopontin, CD44, osteonectin, and alpha-tubulin," *Annals of The New York Academy of Sciences*, vol. 1090, no. 1, pp. 311–317, 2006.

[54] H. Qosa, D. S. Miller, P. Pasinelli, and D. Trotti, "Regulation of ABC efflux transporters at blood-brain barrier in health and neurological disorders," *Brain Research*, vol. 1628, pp. 298–316, 2015.

[55] H. Zhang, X. Zhang, X. Wu et al., "Interference of Frizzled 1 (FZD1) reverses multidrug resistance in breast cancer cells through the Wnt/β-catenin pathway," *Cancer Letters*, vol. 323, no. 1, pp. 106–113, 2012.

[56] M. Flahaut, R. Meier, A. Coulon et al., "The Wnt receptor FZD1 mediates chemoresistance in neuroblastoma through activation of the Wnt/β-catenin pathway," *Oncogene*, vol. 28, no. 23, pp. 2245–2256, 2009.

[57] V. E. Wotring, *Space Pharmacology*, SpringerBriefs in Space Development, New York, NY, USA, 2012.

[58] C. Shende, W. Smith, C. Brouillette, and S. Farquharson, "Drug stability analysis by Raman spectroscopy," *Pharmaceutics*, vol. 6, no. 4, pp. 651–662, 2014.